

Atmospheric correction of ocean color sensors: analysis of the effects of residual instrument polarization sensitivity

Howard R. Gordon, Tao Du, and Tianming Zhang

We provide an analysis of the influence of instrument polarization sensitivity on the radiance measured by spaceborne ocean color sensors. Simulated examples demonstrate the influence of polarization sensitivity on the retrieval of the water-leaving reflectance ρ_w . A simple method for partially correcting for polarization sensitivity—replacing the linear polarization properties of the top-of-atmosphere reflectance with those from a Rayleigh-scattering atmosphere—is provided and its efficacy is evaluated. It is shown that this scheme improves ρ_w retrievals as long as the polarization sensitivity of the instrument does not vary strongly from band to band. Of course, a complete polarization-sensitivity characterization of the ocean color sensor is required to implement the correction. © 1997 Optical Society of America

1. Introduction

The spectral reflectance of the ocean-atmosphere system is modified by the concentration of marine phytoplankton, microscopic plants that constitute the first link in the marine food chain.¹ The component of the spectral reflectance that is caused by photons backscattered out of the ocean (the water-leaving reflectance) is usually termed the ocean color. The flight of the Coastal Zone Color Scanner^{2,3} on the Nimbus-7 satellite proved the feasibility of measuring the concentration of the photosynthetic pigment chlorophyll *a* (a surrogate for the concentration of phytoplankton in the water) on a global scale. On the basis of the success of the coastal zone color scanner, several follow-on ocean color missions have been planned, e.g., the sea-viewing wide-field-of-view sensor (SeaWiFS)⁴ and the moderate-resolution imaging spectroradiometer (MODIS).⁵

The contribution of the water-leaving reflectance ρ_w to the reflectance of the ocean-atmosphere system ρ_t is $\leq 10\%$; the remainder is caused by photons scattered by the atmosphere and reflected from the sea surface. Extraction of ρ_w from ρ_t is referred to as

atmospheric correction. As ρ_w is a small component of ρ_t , adequate atmospheric correction can be effected only if ρ_t is accurately measured, e.g., a 5% error in ρ_t translates into an $\sim 50\%$ error in ρ_w in the blue in waters with low phytoplankton concentrations and a larger error in waters with higher concentrations. The goal set for SeaWiFS and MODIS is the retrieval of ρ_w in such waters with an uncertainty of $\pm 5\%$.

In ocean color remote sensing it is assumed implicitly that the sensor is able to measure accurately (subject to calibration limitations⁶) the radiance that exits the top of the atmosphere (TOA). However, the radiance reflected from the ocean-atmosphere system can be strongly polarized.⁷ Because all radiometers display some sensitivity to the polarization state of the radiance they intend to measure, generally a biased measurement will be obtained. Although the ocean-viewing radiometers are generally designed to have low polarization sensitivity, e.g., for SeaWiFS and MODIS it was specified that the response vary by $< 2\%$ for all linear polarization states of the incident radiance, some may not meet the design requirements. Others, e.g., the spectroscopic imagers on the Midcourse Space Experiment,⁸ were not specifically designed to examine strongly polarized sources and may be quite sensitive to polarization. For this reason, it is of interest to understand the influence of residual instrument polarization sensitivity on the retrieved products and to devise a method to minimize it. This is the focus of this research.

The authors are with Department of Physics, University of Miami, P. O. Box 248046, Coral Gables, Florida 33124.

Received 6 January 1997; revised manuscript received 24 April 1997.

0003-6935/97/276938-11\$10.00/0

© 1997 Optical Society of America

Table 1. Frequently Used Symbols

Symbol	Definition
F_0	Extraterrestrial solar irradiance
\mathbf{I}	Stokes vector with components I , Q , U , and V
\mathbf{I}_t	Stokes vector exiting TOA with components I_t , Q_t , U_t , and V_t
\mathbf{I}_m	TOA Stokes vector measured by the polarization-sensitive instrument
\mathbf{I}_w	Stokes vector exiting the water
\mathbf{M}	Mueller matrix of the instrument's optical system
M_{ij}	Component of \mathbf{M}
m_{ij}	M_{ij}/M_{11}
q	Q/I
u	U/I
P	Degree of polarization associated with \mathbf{I}
\mathbf{P}	Scattering phase matrix
t	Atmospheric diffuse transmittance
α	Angle between the standard reference plane and the instrument's reference plane
ρ	Reflectance: $\pi I/F_0 \cos \theta_0$
ρ_w	Water-leaving reflectance
$\Delta\rho$	Error in retrieved $t\rho_w$
ϕ_v	Relative (to Sun) azimuth of the view direction
θ_v	Sensor viewing angle with respect to the zenith
θ_0	Solar zenith angle
τ_a	Aerosol optical thickness

We review the measurements required to specify the polarization sensitivity of a radiometer, show how the measured TOA radiance depends on the polarization state of the light, and provide examples of the polarization properties of the TOA radiance. Next we review the atmospheric correction algorithm and use it to derive the desired water-leaving radiance by operating it with the radiance measured by the sensor if the instrument's polarization sensitivity is ignored. Finally, we propose a simple algorithm for making an approximate correction for the effects of residual instrument polarization sensitivity and provide some examples of its efficacy.

2. Polarization Sensitivity

A. Sensor Polarization Sensitivity

We assume that the radiometer can be modeled as an optical system that responds in a manner dependent on the state of polarization of the radiance to be measured, and a detector with a response that is independent of the state of polarization of the radiance. The radiance is specified by the column vector \mathbf{I} , the Stokes vector,⁹⁻¹²

$$\begin{pmatrix} I \\ Q \\ U \\ V \end{pmatrix},$$

where

$$\begin{aligned} I &= \langle E_l E_l^* + E_r E_r^* \rangle, \\ Q &= \langle E_l E_l^* - E_r E_r^* \rangle, \\ U &= \langle E_l E_r^* + E_r E_l^* \rangle, \\ V &= i \langle E_l E_r^* - E_r E_l^* \rangle, \end{aligned} \quad (1)$$

E_l and E_r are the components of the electric field in any two orthogonal directions normal to the direction of propagation, the superscript asterisk indicates the complex conjugate, and the angle bracket denotes the average over time. (See Table 1 for symbol descriptions.) The first element of the Stokes vector, I , is the radiance that would be measured with a detector that is insensitive to the polarization state of the field. We refer to it here as the radiance. The polarization state of the radiation is determined by the other components of \mathbf{I} , for example, the degree of polarization of the radiation is

$$P = \frac{(Q^2 + U^2 + V^2)^{1/2}}{I}, \quad (2)$$

where $0 \leq P \leq 1$. The limit $P = 0$ corresponds to a completely unpolarized radiation field, while $P = 1$ corresponds to a completely polarized radiation field. Radiation fields with intermediate values of P are partially polarized. Any field with a degree of polarization P can be represented as a linear combination of an unpolarized field of radiance $(1 - P)I$ and a completely polarized field of radiance PI , i.e.,

$$\mathbf{I} = \begin{pmatrix} I \\ Q \\ U \\ V \end{pmatrix} = \begin{pmatrix} (1 - P)I \\ 0 \\ 0 \\ 0 \end{pmatrix} + \begin{pmatrix} PI \\ Q \\ U \\ V \end{pmatrix}.$$

Fields for which $V = 0$ are considered linearly polarized.

The action of the optical system on \mathbf{I} is to produce a new Stokes vector \mathbf{I}_m given by

$$\mathbf{I}_m = \mathbf{M}\mathbf{I},$$

where \mathbf{M} is a 4×4 matrix (the Mueller matrix). The measured radiance I_m is the top element of the column vector \mathbf{I}_m . The transform matrix \mathbf{M} describes the action of the instrument on \mathbf{I} . It follows from the action of the instrument on the fields,

$$\begin{pmatrix} E_r \\ E_l \end{pmatrix}_m = \mathbf{A} \begin{pmatrix} E_r \\ E_l \end{pmatrix} = \begin{pmatrix} A_1 & A_4 \\ A_3 & A_2 \end{pmatrix} \begin{pmatrix} E_r \\ E_l \end{pmatrix}, \quad (3)$$

where E_r and E_l are the electric field components of the beam in the directions perpendicular and parallel to a reference plane, respectively. This reference plane is arbitrary and is defined with the basis vectors \hat{r} and \hat{l} , respectively perpendicular and parallel to the reference plane. The plane itself is formed by \hat{l} and the direction of propagation of the radiance, $\hat{r} \times \hat{l}$. Starting from Eq. (3) and the definition of I , Q , U , and V in terms of the fields, the derivation of \mathbf{M} from \mathbf{A} is straightforward.^{9,13} In what follows we omit the explicit dependence of \mathbf{I} and \mathbf{M} on wavelength λ for simplicity.

While it views the Earth, the sensor responds to the Stokes vector \mathbf{I}_t exiting the TOA. It is defined with respect to a reference plane determined by the propagation direction of the light (specified by the polar angles θ , ϕ) and the vertical, with \hat{l}_t and \hat{r}_t parallel and perpendicular, respectively, to this plane. However, the transformation matrix \mathbf{M} is defined relative to a reference plane (\hat{l} and \hat{r}) fixed with respect to the instrument. If these two reference planes are not coincident, a transformation (rotation) of the Stokes vector from one reference plane to the other has to be made. By letting $\hat{l}_t \cdot \hat{l} = \cos \alpha$, we have¹³

$$\mathbf{I}_m = \mathbf{MR}(\alpha)\mathbf{I}_t, \quad (4)$$

where

$$\mathbf{R}(\alpha) \equiv \begin{pmatrix} 1 & 0 & 0 & 0 \\ 0 & \cos 2\alpha & \sin 2\alpha & 0 \\ 0 & -\sin 2\alpha & \cos 2\alpha & 0 \\ 0 & 0 & 0 & 1 \end{pmatrix},$$

with α measured clockwise from \hat{l}_t to \hat{l} looking toward the source. Equation (4) shows that the instrument—the optical system that changes \mathbf{I}_t into \mathbf{I}_m and the detector that responds only to I_m —measures an I_m that is related to the components of the true Stokes vector \mathbf{I}_t by

$$I_m = M_{11}I_t + M_{12}(\cos 2\alpha Q_t + \sin 2\alpha U_t) + M_{13}(-\sin 2\alpha Q_t + \cos 2\alpha U_t) + M_{14}V_t, \quad (5)$$

where M_{11} , M_{12} , M_{13} , and M_{14} are the elements of the first row of the matrix \mathbf{M} . For the radiance back-scattered to the top of the atmosphere, $V_t \approx 0$ (refer to Subsection 2.B), so I_m in Eq. (5) can be rewritten as

$$I_m = M_{11}I_t + M_{12}(\cos 2\alpha Q_t + \sin 2\alpha U_t) + M_{13}(-\sin 2\alpha Q_t + \cos 2\alpha U_t). \quad (6)$$

It is clear the measured radiance I_m is not I_t ; I_m depends on the characteristics of the instrument (M_{11} , M_{12} , and M_{13}) and the characteristics of the radiation (I_t , Q_t , and U_t). Of course, it is desirable to have an ideal instrument with no polarization sensitivity, i.e., $M_{ij} = 0$ for $i > 1$ and $j > 1$; however, this is not practical. On one hand, all instruments have some unavoidable polarization sensitivity. On the other hand, if the degree of polarization of the radiance received by the instrument is zero ($Q_t = U_t = V_t = 0$), the measured radiance I_m will be the true radiance I_t . However, because the upwelling radiance we intend to measure is polarized, I_m will never be I_t .

To study the effect of the polarization sensitivity of the instrument, we need to know only three elements, M_{11} , M_{12} , and M_{13} , in the transform matrix \mathbf{M} . These can be determined with standard measurements,¹² which we review here. First, choose a reference plane for the instrument, with basis vectors \hat{l} and \hat{r} parallel and perpendicular to this reference plane, respectively, and $\hat{r} \times \hat{l}$ in the propagation direction of the beam. Then illuminate the instrument with linearly polarized radiance ($P = 1$) of radiance I_0 in the following ways [to conserve space we write \mathbf{I} as a row vector, $\mathbf{I} = (I, Q, U, V)$].

(1) With the oscillation direction (plane) of the electric vector along \hat{l} , so the incident Stokes vector is $\mathbf{I}_{in} = I_0(1, 1, 0, 0)$, for which the instrument records a radiance I_i , and from Eq. (6) with $\alpha = 0$ (since M_{11} , M_{12} , and M_{13} are defined on this reference plane) we have

$$I_i = (M_{11} + M_{12})I_0.$$

(2) With the oscillation direction along \hat{r} , i.e., $\mathbf{I}_{in} = I_0(1, -1, 0, 0)$, for which the instrument records a radiance I_r , we have

$$I_r = (M_{11} - M_{12})I_0.$$

(3) With the oscillation direction along the line that bisects the angle between \hat{l} and \hat{r} , i.e., $\mathbf{I}_{in} = I_0(1, 0, 1, 0)$, for which the instrument records a radiance $I_{i\hat{r}}$, we have

$$I_{i\hat{r}} = (M_{11} + M_{13})I_0.$$

From these experimental results, M_{11} , M_{12} , and M_{13} can be found easily:

$$M_{11} = \frac{I_i + I_r}{2I_0},$$

$$M_{12} = \frac{I_i - I_r}{2I_0},$$

$$M_{13} = \frac{I_{i\hat{r}}}{I_0} - M_{11}.$$

Considering that M_{11} can be determined with an unpolarized source during instrument calibration, we

use $M_{11} = 1$ in this research. Upon defining q_t and u_t as

$$q_t = \frac{Q_t}{I_t},$$

$$u_t = \frac{U_t}{I_t},$$

Eq. (6) can be rewritten

$$I_m = I_t[1 + m_{12}(\cos 2\alpha q_t + \sin 2\alpha u_t) + m_{13}(-\sin 2\alpha q_t + \cos 2\alpha u_t)], \quad (7)$$

with m_{12} and m_{13} defined by

$$m_{12} = \frac{M_{12}}{M_{11}},$$

$$m_{13} = \frac{M_{13}}{M_{11}}.$$

Even if I_0 is unknown in the above experiment, we can obtain the polarization sensitivity of instrument by finding m_{12} and m_{13} from the following equations:

$$m_{12} = \frac{I_l - I_r}{I_l + I_r},$$

$$m_{13} = \frac{2I_{lr}}{I_l + I_r} - 1.$$

B. Polarization Properties of I_t

To examine the influence of the instrument polarization sensitivity, we need to know the polarization characteristics of the radiance that exits the TOA. For remote sensing of ocean color, in general, I_t can be written as

$$I_t = I_r + I_a + I_{ra} + tI_w, \quad (8)$$

where I_r is the contribution from the Rayleigh scattering, I_a is the contribution from the aerosol scattering, I_{ra} is the contribution from the interaction between molecular and aerosol scattering, tI_w is the water-leaving radiance diffusely transmitted (t) to the top of the atmosphere. This yields

$$I_t = I_r + I_a + I_{ra} + tI_w.$$

The water-leaving component tI_w is at most (in the blue) $\sim 10\%$ of the total I_t ; and if we consider the incident light field on the TOA from the Sun is completely unpolarized, the polarization state of I_t is governed mainly by the atmospheric scattering contribution. For Rayleigh scattering, the I_t polarization state is well known and easy to determine; but for aerosols, the scattering properties and the polarization state of the scattered light are generally unknown because they depend strongly on their particle size distributions and refractive indices.

Consider a spherical coordinate system with origin at the TOA, z axis directed downward, and x axis directed away from the Sun (Sun's rays are in the $x-z$

plane). Let the direction of propagation of a photon be specified by the polar and azimuth angles, θ and ϕ , in this system. The solar beam has $\theta = \theta_0$ and $\phi = 0$. Photons exiting the TOA have $\theta > 90^\circ$. With τ representing the optical depth measured from the TOA, the propagation of \mathbf{I} at a wavelength λ is governed by the vector radiative transfer equation (VRTE),

$$\cos \theta \frac{d\mathbf{I}(\lambda, \tau, \theta, \phi)}{d\tau} = -\mathbf{I}(\lambda, \tau, \theta, \phi) + \omega_0 \int_{4\pi} \mathbf{R}(\alpha)\mathbf{P}(\lambda, \tau, \theta', \phi' \rightarrow \theta, \phi) \times \mathbf{R}'(\alpha')\mathbf{I}(\lambda, \tau, \theta', \phi')d\Omega', \quad (9)$$

where \mathbf{P} is the phase matrix, ω_0 is the single-scattering albedo, and \mathbf{R} is the rotation matrix. In Subsection 2.A, the reference plane for \mathbf{I} is defined by the direction of propagation and the z axis, i.e., the reference plane, is perpendicular to the ocean surface. Note that there are two rotations among three reference planes whenever a scattering occurs¹⁰ because the phase matrix is defined on the scattering plane (determined by the incident light and the scattered light). One must first rotate the incident reference plane to the scattering plane, then apply phase matrix \mathbf{P} , and finally rotate the scattering plane to the scattered reference plane. The boundary condition at the TOA is

$$\mathbf{I}(0; \theta, \phi) = \begin{pmatrix} F_0 \\ 0 \\ 0 \\ 0 \end{pmatrix} \delta(\cos \theta - \cos \theta_0) \times \delta(\phi - \phi_0), \quad \theta_0 < \pi/2.$$

The boundary condition at the (assumed flat) sea surface is given by

$$\mathbf{I}(\tau_1; \theta_r, \phi_r) = \mathbf{F}(\theta_i)\mathbf{I}(\tau_1; \theta_i, \phi_i), \quad (10)$$

where the Fresnel reflection Mueller matrix \mathbf{F} is

$$\mathbf{F}(\theta_i) = \begin{bmatrix} \rho + (\theta_i) & \rho - (\theta_i) & 0 & 0 \\ \rho - (\theta_i) & \rho + (\theta_i) & 0 & 0 \\ 0 & 0 & \rho_{33}(\theta_i) & 0 \\ 0 & 0 & 0 & \rho_{33}(\theta_i) \end{bmatrix}, \quad (11)$$

with $\theta_r = \pi - \theta_i$ and $\phi_r = \phi_i$. The factors $\rho \pm (\theta_i)$ and $\rho_{33}(\theta_i)$ are given by

$$\rho \pm (\theta_i) = \frac{1}{2} \left[\frac{\cos \theta_i - (n^2 - \sin^2 \theta_i)^{1/2}}{\cos \theta_i + (n^2 - \sin^2 \theta_i)^{1/2}} \right]^2 \times \left\{ \left[\frac{\sin^2 \theta_i - \cos \theta_i (n^2 - \sin^2 \theta_i)^{1/2}}{\sin^2 \theta_i + \cos \theta_i (n^2 - \sin^2 \theta_i)^{1/2}} \right]^2 \pm 1 \right\},$$

$$\rho_{33}(\theta_i) = \left[\frac{\cos \theta_i - (n^2 - \sin^2 \theta_i)^{1/2}}{\cos \theta_i + (n^2 - \sin^2 \theta_i)^{1/2}} \right]^2 \times \left[\frac{\sin^2 \theta_i - \cos \theta_i (n^2 - \sin^2 \theta_i)^{1/2}}{\sin^2 \theta_i + \cos \theta_i (n^2 - \sin^2 \theta_i)^{1/2}} \right].$$

The aerosol-scattering phase matrix has the following form for spherical particles:

$$\mathbf{P}_a(\Theta) = \begin{pmatrix} P_{11} & P_{12} & 0 & 0 \\ P_{12} & P_{11} & 0 & 0 \\ 0 & 0 & P_{33} & P_{34} \\ 0 & 0 & -P_{34} & P_{33} \end{pmatrix}, \quad (12)$$

where P_{11} , P_{12} , P_{33} , and P_{34} are functions of the scattering angle Θ . For the aerosol models used in this study, the phase matrices are computed with the Mie theory. The Rayleigh phase matrix, \mathbf{P}_r , is

$$\mathbf{P}_r(\Theta) = \frac{3}{16\pi} \begin{pmatrix} 1 + \cos^2 \Theta & -\sin^2 \Theta & 0 & 0 \\ -\sin^2 \Theta & 1 + \cos^2 \Theta & 0 & 0 \\ 0 & 0 & 2 \cos \Theta & 0 \\ 0 & 0 & 0 & 2 \cos \Theta \end{pmatrix}, \quad (13)$$

where Θ is the scattering angle. Note that the depolarization factor¹⁴ has been set to 0.

The VRTE can be solved by the successive order method and the Monte Carlo method, similar to the scalar radiative transfer equation. However, instead of solving a single equation in the scalar radiative transfer equation approximation, we must solve four coupled equations.

Although the upwelling radiance I_t at the TOA is not the result of just single scattering, we gain some understanding by examining the Rayleigh and aerosol single-scattering contributions to I_t . From single-scattering theory, with the incident light on TOA completely unpolarized, the upwelling radiance that exits the TOA by direct molecular or aerosol scattering (i.e., without the reflection from the ocean surface considered) is given by¹⁴

$$\begin{pmatrix} I_t \\ Q_t \\ U_t \\ V_t \end{pmatrix} = \frac{F_0 \cos \theta_0 \omega_0}{\cos \theta_0 - \cos \theta} \left[1 - \exp\left(\frac{\tau_1}{\cos \theta} - \frac{\tau_1}{\cos \theta_0}\right) \right] \times \begin{bmatrix} P_{11}(\Theta) \\ P_{12}(\Theta) \cos 2\alpha \\ -P_{12}(\Theta) \sin 2\alpha \\ 0 \end{bmatrix}, \quad (14)$$

where ω_0 is the single-scattering albedo, τ_1 is the optical thickness of the molecules or aerosols, and Θ is the scattering angle. Note that there is no contribution to V_t from single Rayleigh scattering or single aerosol scattering. With the observation that there is no P_{34} term in the Rayleigh-scattering phase matrix, there is no contribution to V_t from pure Rayleigh multiple scattering either. The term V_t is the result either of multiple aerosol scattering (including the aerosol and Rayleigh interaction terms) because of the existence of element P_{34} in the scattering phase matrix of aerosols or of single scattering followed by or preceded by reflection from the sea surface. Our

simulation results agree with the computations of Kattawar *et al.*¹⁵ and Plass *et al.*¹⁶ that $V_t \approx (V_a + V_{ra}) \sim 10^{-3} I_t$, which is why we can assume $V_t \approx 0$ in Eq. (6). This means circular polarization effects are ignored.

From Eq. (14) we can also see that, in the case of single scattering, Q and U (or the degree of polarization) are introduced mainly because of the existence of the scattering phase matrix element P_{12} for Rayleigh and aerosol scattering. Figure 1 provides P_{12} for Rayleigh scattering and aerosol scattering as a function of scattering angle Θ . The aerosol models used in Fig. 1 are the Shettle and Fenn¹⁷ maritime and tropospheric models at 80% relative humidity, labeled as M80 and T80 respectively. It is observed from Fig. 1 that P_{12} for the aerosol is usually small compared with that for Rayleigh scattering and that this element for Rayleigh scattering is a strong function of the scattering angle Θ . In the backward directions ($90^\circ < \Theta \leq 180^\circ$), when Θ is greater than $\sim 160^\circ$, the P_{12} elements for Rayleigh and aerosol scattering are comparable. In contrast, when $90^\circ < \Theta \leq 150^\circ$, Rayleigh scattering has a strong effect on the polarization state. Thus when single scattering dominates, the degree of polarization will be small for large scattering angle Θ ($\Theta > 160^\circ$), but when Θ is less than 150° , strong polarization effects caused largely by Rayleigh scattering will be encountered.

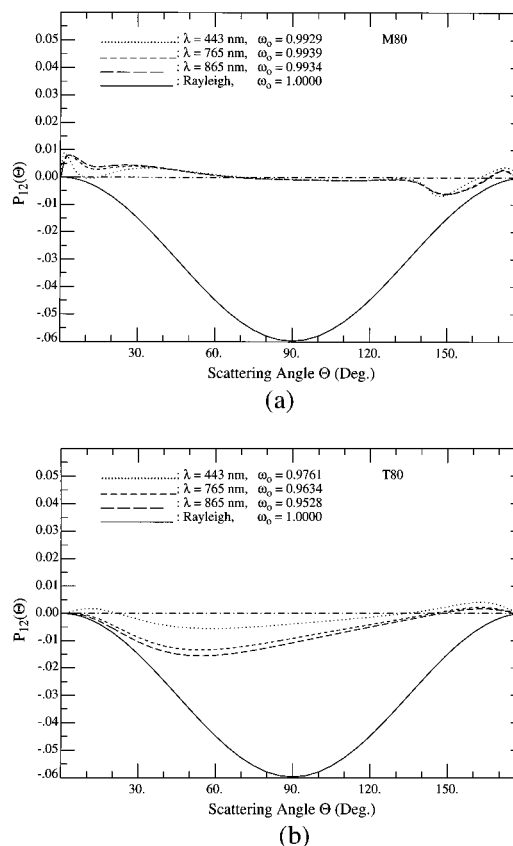


Fig. 1. Scattering phase matrix element P_{12} for aerosols at 443, 765, and 865 nm, and Rayleigh: (a) M80 aerosol model and (b) T80 aerosol model.

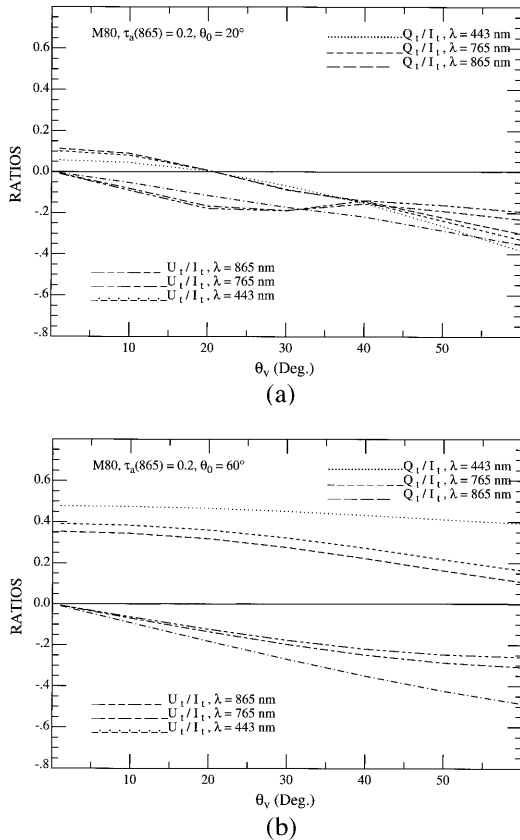


Fig. 2. Ratios Q_t/I_t and U_t/I_t as a function of θ_v for the M80 aerosol model with $\phi = 90^\circ$: (a) $\theta_0 = 20^\circ$ and (b) $\theta_0 = 60^\circ$.

By using the aerosol models described by Gordon and Wang,¹⁸ one can compute the Stokes vector \mathbf{I}_t by solving the VRTE. By using a two-layer atmosphere model with molecules confined in the upper layer and aerosols confined in the lower layer bounded by a flat Fresnel-reflecting ocean surface, we solved the VRTE with a Monte Carlo code to provide a pseudoradiance vector \mathbf{I}_t received by the sensor at the TOA. The simulations we present were carried out for the M80 and T80 aerosol models in three wave bands (443, 765, and 865 nm), and the aerosol optical thickness for $\lambda = 865$ nm was taken to be 0.2 [$\tau_a(865) = 0.2$].

Because the error in I_m [Eq. (7)] is determined by q_t and u_t , the ratios of Q_t/I_t and U_t/I_t computed for M80 at three wavelengths are plotted in Fig. 2 as a function of the viewing angle of the sensor, $\theta_v \equiv \pi - \theta$, for $\phi = 90^\circ$. The T80 aerosol model yields similar curves. Note that U_t changes sign upon crossing the principal plane ($\phi = 0$). In Fig. 2 we plot U_t for the side of the principal plane for which it is negative. In contrast, Q_t is symmetric with respect to reflection across the principal plane. These computations show that (1) the degree of polarization P generally increases with increasing θ_0 and θ_v ; (2) P can be as large as ~ 0.5 – 0.6 ; (3) both Q_t and U_t contribute significantly to P (Q_t for small θ_v and U_t for large θ_v); and (4) the polarization properties at 765 and 865 nm are similar but show significantly less polarization than at 443 nm.

These computations can be used to obtain a coarse estimate of the error in I_t , induced by the polarization sensitivity. Choose \hat{l} and \hat{r} so that $m_{13} = 0$. Then

$$\frac{\Delta I_t}{I_t} \equiv \frac{I_m - I_t}{I_t} = m_{12}(q_t \cos 2\alpha + u_t \sin 2\alpha).$$

It is easy to show that the maximum value of $(q_t \cos 2\alpha + u_t \sin 2\alpha)$ is $P_l \equiv (q_t^2 + u_t^2)^{1/2}$. Thus

$$\frac{\Delta I_t}{I_t} \leq m_{12}P_l.$$

As P_l can be as large as 0.5–0.6, we see that the error in I_t is potentially as large as $\sim 0.5m_{12}$. For $m_{12} \leq 0.02$, the error is at most 1%. In contrast, if $m_{12} = 0.10$, the error could be as large as 5%. Gordon¹⁹ showed that errors of 1% can be tolerated in atmospheric correction as long as the error has the same sign throughout the spectrum; however, errors of $\sim 5\%$ cannot be tolerated.

3. Effects of Sensor Polarization Sensitivity on Atmospheric Correction

In the absence of strongly absorbing aerosols and instrument polarization sensitivity, the Gordon and Wang atmospheric correction algorithm works well.¹⁹ The error in the retrieved water-leaving reflectance at 443 nm $\Delta\rho(443) = t(443)\Delta\rho_w(443)$, where the reflectance $\rho_w \equiv \pi I_w/F_0 \cos \theta_0$, is approximately ± 0.001 to ± 0.002 . This meets the requirements of MODIS and SeaWiFS. However, because the instrument has a residual polarization sensitivity and the upwelling radiance I_t we intend to measure is polarized, we cannot be provided with the true I_t . Instead we will have the biased I_m . Therefore it is necessary to assess the influence of polarization sensitivity on the Gordon and Wang atmospheric correction algorithm.

We used simulated \mathbf{I}_m pseudodata to study the influence of the polarization sensitivity of the instrument on the performance of the Gordon and Wang atmospheric correction algorithm. \mathbf{I}_t was computed for the M80 and T80 aerosol models with aerosol optical thickness at 865 nm, $\tau_a(865) = 0.2$. This value of $\tau_a(865)$ is somewhat higher than that observed over regions with a pure maritime atmosphere, i.e., not subjected to anthropogenic aerosol or mineral dust transported over the oceans.^{20–22} The water-leaving radiance was taken to be 0. The simulations were carried out for $\theta_0 = 0, 20^\circ, 40^\circ$, and 60° , both at the center, $\theta_v \approx 1^\circ$, and at the edge, $\theta_v \approx 45^\circ$, of the SeaWiFS scan with $\phi = 90^\circ$. The combination $\theta_0 = 0$ and $\theta_v \approx 1^\circ$ is omitted because it would be near the center of the Sun's glitter pattern. These seven geometries cover approximately the full range of Sun-view geometries encountered in progressing along a polar orbit from the equator to a latitude of 60° at the equinox.

The Stokes vector \mathbf{I}_t was then introduced into Eq. (7) and I_m computed, given the polarization sensitivity of the sensor. A rotation of the reference plane used to define m_{12} and m_{13} does not change $(m_{12}^2 +$

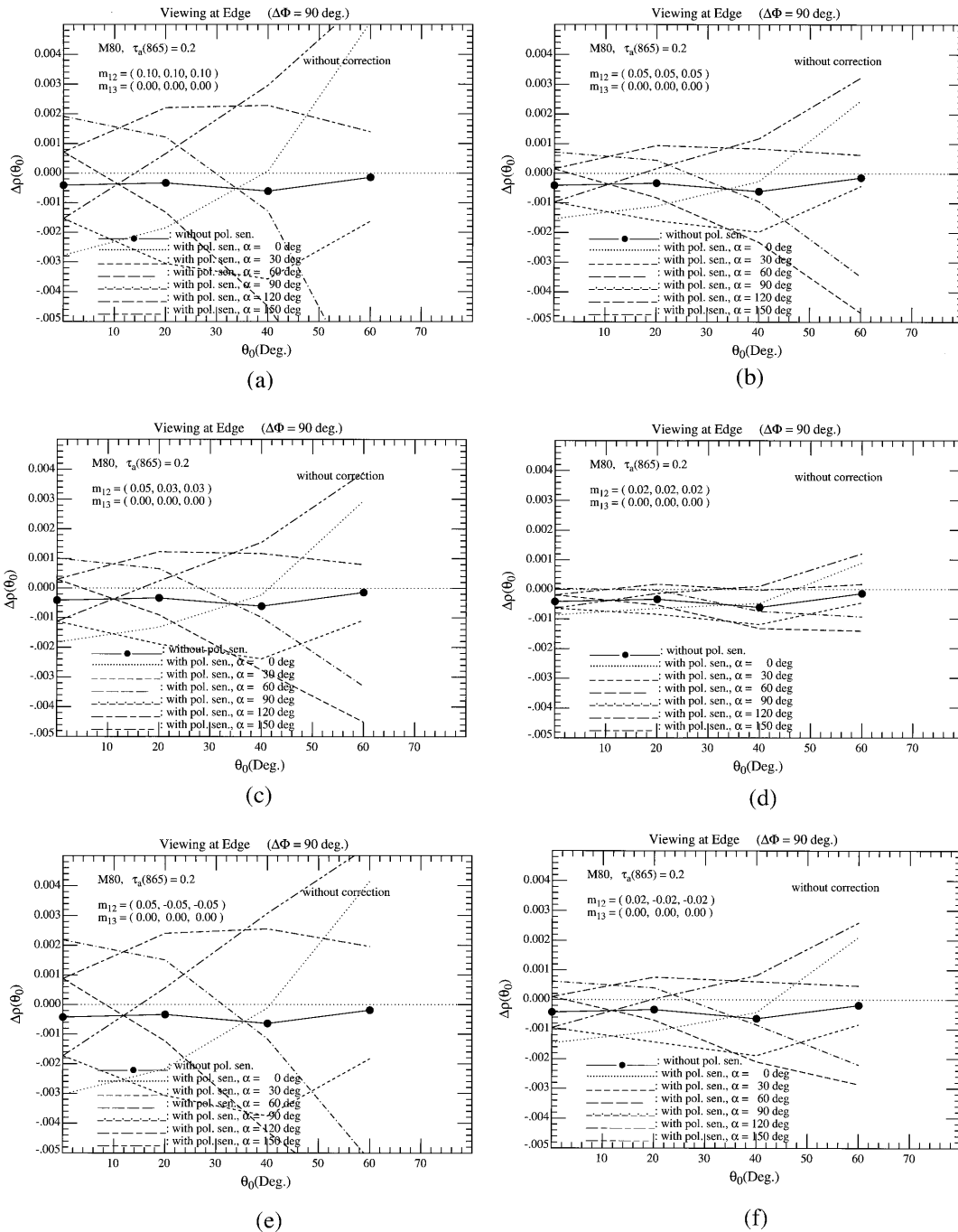


Fig. 3. Retrieved error $t\Delta\rho_w$ at 443 nm as a function of θ_0 for the M80 aerosol model with $\tau_a(865) = 0.2$, in the presence of polarization sensitivity, for viewing at the edge of the scan with (a) $m_{12} = (0.10, 0.10, 0.10)$; (b) $m_{12} = (0.05, 0.05, 0.05)$; (c) $m_{12} = (0.05, 0.03, 0.03)$; (d) $m_{12} = (0.02, 0.02, 0.02)$; (e) $m_{12} = (0.05, -0.05, -0.05)$; (f) $m_{12} = (0.02, -0.02, -0.02)$.

$m_{13}^2)^{1/2}$; it only reallocates polarization sensitivity between m_{12} and m_{13} , i.e., it simply changes the definition of the angle α . Thus, for simplicity, we set m_{13} equal to 0 and present the results of our study as a function of α .

The Gordon and Wang algorithm¹⁸ uses the SeaWiFS bands at 765 and 865 nm (where $\rho_w = 0$, except in turbid coastal water) to provide atmospheric correction for the visible. Here we examine the error in the water-leaving reflectance, $t\Delta\rho_w \equiv \Delta\rho$, at 443 nm.

To demonstrate the effect of the polarization sensitivity, we examined six sets of values of m_{12} in the three wave bands of 443, 765, and 865 nm. The six sets of m_{12} {written [$m_{12}(443), m_{12}(765), m_{12}(865)$]} were $m_{12} = (0.10, 0.10, 0.10)$, $m_{12} = (0.05, 0.05, 0.05)$, $m_{12} = (0.05, 0.03, 0.03)$, $m_{12} = (0.02, 0.02, 0.02)$, $m_{12} = (0.05, -0.05, -0.05)$, and $m_{12} = (0.02, -0.02, -0.02)$. As mentioned in the preceding paragraph, $m_{13} = (0, 0, 0)$ for each set. Note that setting m_{13} to 0 at all three wave bands implies that when the plane of

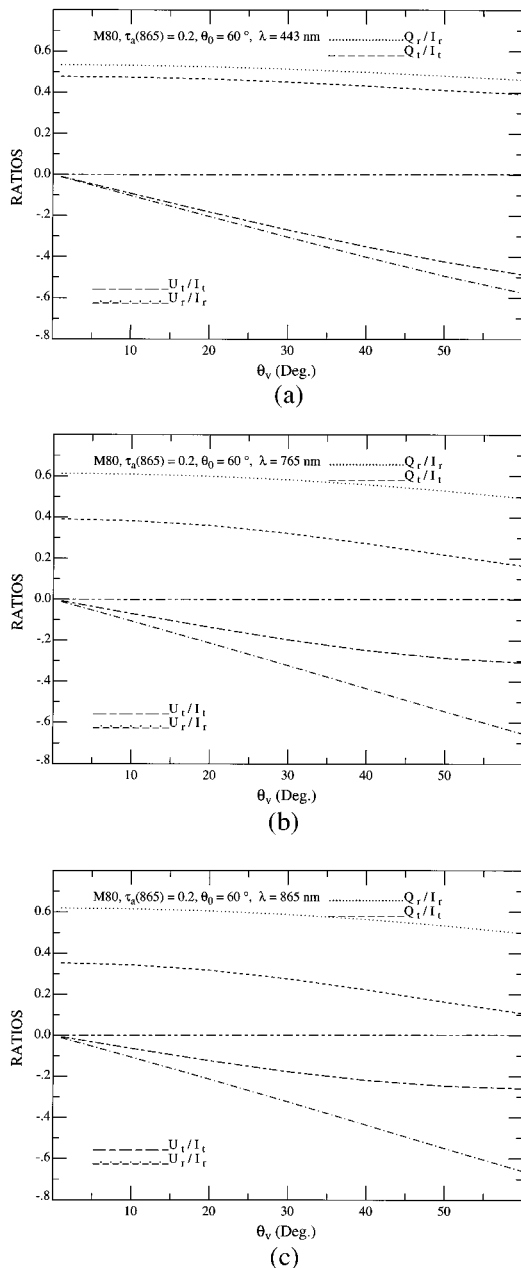


Fig. 4. Ratios Q/I and U/I for Rayleigh scattering and total scattering as a function of viewing zenith angle θ_v for the M80 aerosol model with $\tau_a(865) = 0.2$ and $\theta_0 = 60^\circ$: (a) $\lambda = 443$ nm; (b) $\lambda = 765$ nm; (c) $\lambda = 865$ nm.

polarization of radiation (of constant radiance) entering the sensor is rotated through 360° , the sinusoidal responses (in $2 \times$ the rotation angle) of the detectors for the three bands will be either in phase or exactly out of phase with each other. This is not a necessity for the development we present; it is used only to simplify the analysis.

Sample results for the errors in the retrieved water-leaving reflectance at 443 nm are presented in Fig. 3 for viewing at the scan edge with $\phi = 90^\circ$, as a function of α . For this fixed viewing geometry, α would be constant; however, here varying α is iden-

tical to varying the fraction of the polarization sensitivity allocated to m_{12} and m_{13} . The solid curve that connects the solid dots on Fig. 3 provides the error in $t\rho_w$ in the absence of polarization sensitivity, i.e., the result of operating the algorithm with the correct input, I_t not I_m . The simulation results in Fig. 3 suggest that (1) large instrument m_{12} causes large errors when polarization state is considered; (2) for m_{12} as small as 0.02, the polarization sensitivity effects are not a problem in most Sun-viewing geometries (error $< \pm 0.002$) as long as the m_{12} has the same sign in all bands; (3) retrieval errors for $m_{12} = (0.05, 0.05, 0.05)$ are approximately same as that for $m_{12} = (0.05, 0.03, 0.03)$, and retrieval errors for $m_{12} = (0.05, -0.05, -0.05)$ are approximately the same as that for $m_{12} = (0.10, 0.10, 0.10)$, suggesting that when m_{12} are wavelength dependent, the retrieval errors are larger than those when they are wavelength independent.

It is clear that the performance of the Gordon and Wang algorithm is degraded in the presence of sensor polarization sensitivity. Thus a method to remove the errors induced by the instrument polarization sensitivity is required.

4. Removal of Instrument Polarization Sensitivity

To completely remove the instrument polarization sensitivity, one needs the polarization properties of the upwelling radiance vector I_t . Because aerosol scattering is highly variable, measuring only the upwelling radiance I_t cannot provide any information regarding its polarization characteristics. It is fortunate that the polarization state of the upwelling radiance I_t is determined mainly by Rayleigh scattering (Fig. 1). Figure 4 provides a comparison of Q/I and U/I between Rayleigh scattering (without aerosols) and total scattering (Rayleigh plus aerosols) for $\theta_0 = 60^\circ$. When associated with Q/I and U/I , the subscripts r and t refer to Rayleigh scattering and total scattering, respectively. Figure 4 shows that, generally in the blue, Q_r/I_r is close to Q_t/I_t and U_r/I_r is close to U_t/I_t , with $|Q_r/I_r| > |Q_t/I_t|$ and $|U_r/I_r| > |U_t/I_t|$. This can be explained by the aerosol-scattering contribution to Q_t and U_t being generally smaller than its contribution to I_t , which means the existence of the aerosol reduces the degree of polarization attributed to pure Rayleigh scattering in the upwelling radiance vector I_t . For the short wavelength [Fig. 4(a)] the Rayleigh scattering dominates, and there is little difference between Q_r/I_r and Q_t/I_t and between U_r/I_r and U_t/I_t . For the long wavelengths [Figs. 4(b) and 4(c)] aerosol scattering reduces significantly the degree of polarization of the upwelling radiance.

Observing that a significant portion of q_t and u_t is contributed by Rayleigh scattering and noting that the Rayleigh-scattering properties of the air are well known, we would expect that a significant amount of the polarization-induced error in $t\rho_w(443)$ could be removed by replacing q_t and u_t in Eq. (7) with their Rayleigh-scattering counterparts, Q_r/I_r and U_r/I_r . When q_r is close to q_t and u_r is close to u_t , the cor-

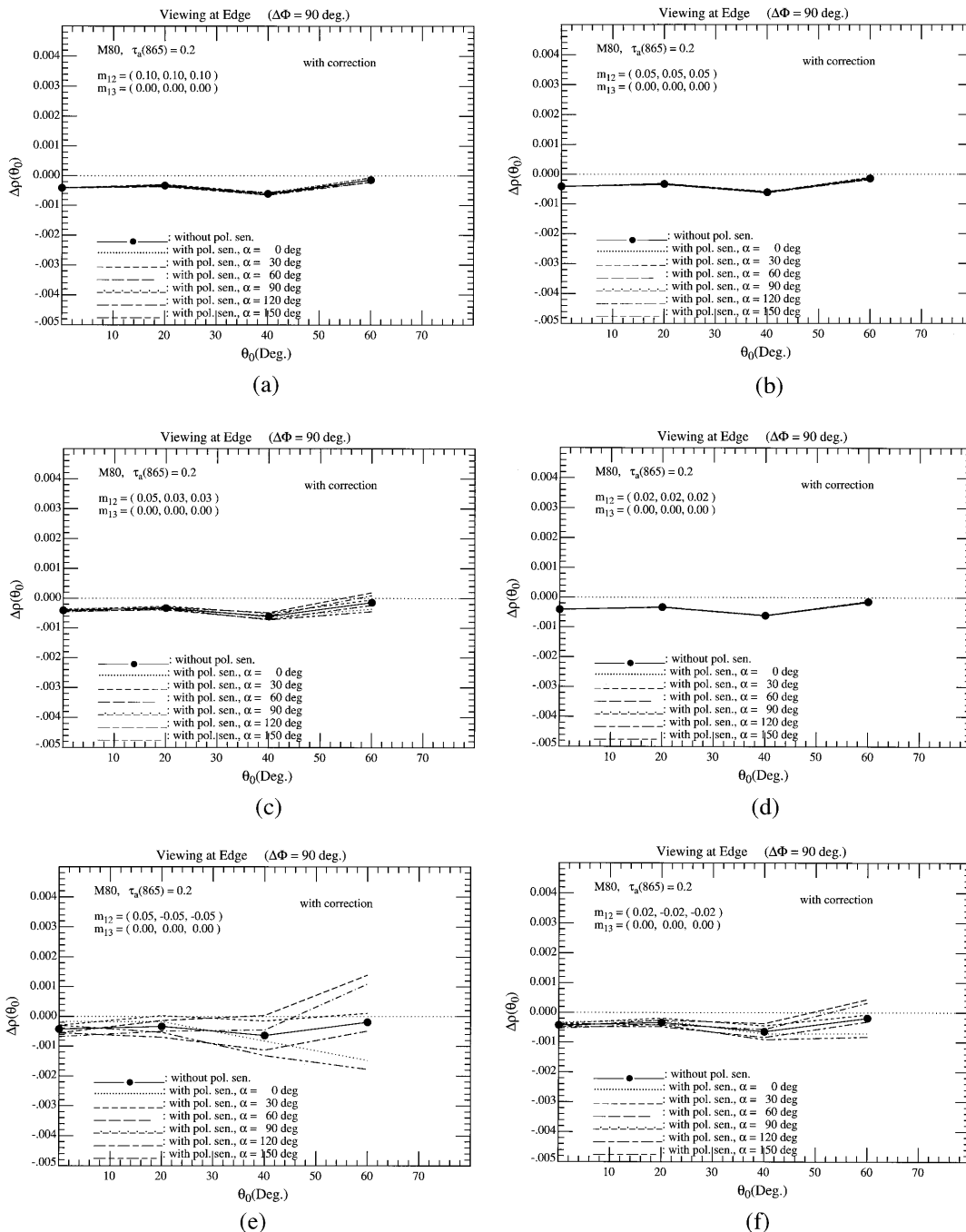


Fig. 5. Retrieved error $t\Delta\rho_w$ at 443 nm as a function of θ_0 for the M80 aerosol model with $\tau_a(865) = 0.2$, after applying the removal algorithm, for viewing at the edge of the scan with (a) $m_{12} = (0.10, 0.10, 0.10)$; (b) $m_{12} = (0.05, 0.05, 0.05)$; (c) $m_{12} = (0.05, 0.03, 0.03)$; (d) $m_{12} = (0.02, 0.02, 0.02)$; (e) $m_{12} = (0.05, -0.05, -0.05)$; (f) $m_{12} = (0.02, -0.02, -0.02)$.

rected radiance should be close to the true radiance I_r . With the upwelling radiance at the TOA corrected in this manner, instead of applying the biased I_m we applied the Gordon and Wang atmospheric correction algorithm to the same pseudodata used in Fig. 3. The retrieved errors in water-leaving reflectance at 443 nm are presented in Fig. 5. Observe from the simulations that (1) generally, the polarization correction works better for smaller m_{12} ; (2) when m_{12} is not dependent on wavelength, it works well even for

m_{12} as large as (0.1, 0.1, 0.1); (3) when m_{12} is dependent on wavelength, it does not work as well as in observation (1); and (4) when values of m_{12} have different signs in different wave bands, even for m_{12} as small as 2%, it cannot perform well [Figs. 5(e) and 5(f)]. Similar results were obtained for the T80 aerosol model with $\tau_a = 0.2$, although the residual error in $t\rho_w$ was larger. For the purpose of removing the effects of polarization sensitivity, these simulations show the importance of designing instruments

in which m_{12} does not significantly depend on wavelength.

We tried to improve on this polarization-sensitivity correction by accounting for the presence of aerosols, which cause the difference between the q_r-u_r pair and the q_t-u_t pair (Fig. 4). However, because the polarization properties of the aerosol cannot be known prior to atmospheric correction, some assumption must be made in this regard. Figure 1 suggests that a reasonable assumption would be that aerosol single scattering depolarizes completely the incident radiance, i.e., that the only nonzero element of $\mathbf{P}_a(\Theta)$ is at the top left of the matrix. In the single-scattering approximation to the TOA radiance, this would correspond to the replacement of the actual q_t with Q_r/I_t and u_t with U_r/I_t . Such a replacement would effect a first-order correction for the depolarization by aerosols. Because I_t is unknown, we tried replacing I_t with I_m , the radiance measured without regard for the polarization sensitivity, i.e., in Eq. (7) we replaced q_t and u_t with Q_r/I_m and U_r/I_m , respectively. The results were disappointing; there was no improvement in the polarization correction, and in many cases the error after correction was larger than that shown in Fig. 5 (but less than that in Fig. 3). Thus we rejected this method in favor of replacing q_t and u_t in Eq. (7) with q_r and u_r , respectively.

In all of the simulations presented here, we took ρ_w to be 0, so the error in $t\rho_w$ was just the value of $t\rho_w$ retrieved by the atmospheric correction algorithm. Of course, $\rho_w \neq 0$ in the visible, and in fact the light that exits the ocean will have its own polarization properties.^{23,24} Thus, if $\rho_w \neq 0$, the polarization properties of \mathbf{I}_t will change, which will produce a concomitant change in \mathbf{I}_m . Although there have been no thorough studies of the polarization properties of the water-leaving reflectance, it is easy to see that the error induced by the polarization of ρ_w will be small. In very clear waters in the blue, I_w typically contributes at most 10% of I_t . Thus if \mathbf{I}_w is fully polarized ($P = 1$) or fully depolarized ($P = 0$), the degree of polarization of \mathbf{I}_t will change by at most 0.1. An analysis similar to that presented at the end of Subsection 2.B shows that such a change in the polarization state of \mathbf{I}_t will induce a change in I_m of at most $m_{12}/10$. Because m_{12} is expected to be small, e.g., <0.05 , the maximum additional error in I_t will be $<0.5\%$ in the blue in clear water. For longer wavelengths I_w is an even smaller component of I_t , so the error there will be even less. In reality, the polarization state of \mathbf{I}_w is likely to be similar to \mathbf{I}_t , in which case there would be no additional error resulting from nonzero values of ρ_w . Thus we believe our simulations with $\rho_w = 0$ provide an adequate estimate of the performance of the correction algorithm in the presence of an instrument with a relatively small polarization sensitivity.

5. Concluding Remarks

We present simulations that demonstrate the effect of sensor polarization sensitivity on the atmospheric correction of ocean color sensors (Fig. 3). In addition,

we provide a simple method—substituting the polarization properties of \mathbf{I}_t with those of a pure Rayleigh-scattering atmosphere—for partially correcting the error induced by polarization sensitivity. This correction method is shown to be effective (even for relatively large polarization sensitivities) as long as the polarization sensitivity of the instrument does not vary strongly from band to band [Fig. 5(a)–5(d)]. An attractive feature of this polarization correction is the simplicity of its implementation as part of the overall atmospheric correction algorithm. The possible error in the retrieved values of $t\rho_w$ without polarization correction (Fig. 3) underscores the importance of a complete characterization of the polarization sensitivity of an ocean color sensor prior to launch so that the polarization-sensitivity correction can be applied.

The authors gratefully acknowledge the National Aeronautics and Space Administration for support under grant NAGW-273 and contracts NAS5-31363 and NAS5-31734.

References

1. H. R. Gordon and A. Y. Morel, *Remote Assessment of Ocean Color for Interpretation of Satellite Visible Imagery: A Review* (Springer-Verlag, New York, 1983).
2. W. A. Hovis, D. K. Clark, F. Anderson, R. W. Austin, W. H. Wilson, E. T. Baker, D. Ball, H. R. Gordon, J. L. Mueller, S. Y. E. Sayed, B. Strum, R. C. Wrigley, and C. S. Yentsch, "Nimbus 7 coastal zone color scanner: system description and initial imagery," *Science* **210**, 60–63 (1980).
3. H. R. Gordon, D. K. Clark, J. L. Mueller, and W. A. Hovis, "Phytoplankton pigments derived from the Nimbus-7 CZCS: initial comparisons with surface measurements," *Science* **210**, 63–66 (1980).
4. S. B. Hooker, W. E. Esaias, G. C. Feldman, W. W. Gregg, and C. R. McClain, "An overview of SeaWiFS and ocean color," in *SeaWiFS Technical Report Series*, Vol. 1, NASA Technical Memorandum 104566, July 1992 (NASA, Greenbelt, Md.).
5. V. V. Salomonson, W. L. Barnes, P. W. Maymon, H. E. Montgomery, and H. Ostrow, "MODIS: advanced facility instrument for studies of the Earth as a system," *IEEE Geosci. Remote Sensing* **27**, 145–152 (1989).
6. H. R. Gordon, "Calibration requirements and methodology for remote sensors viewing the oceans in the visible," *Remote Sensing Environ.* **22**, 103–126 (1987).
7. G. W. Kattawar, G. N. Plass, and J. A. Guinn, "Monte Carlo calculations of the polarization of radiation in the Earth's atmosphere-ocean system," *J. Phys. Oceanogr.* **3**, 353–372 (1973).
8. J. D. Mill, R. R. O'Neil, S. Price, G. J. Romick, O. M. Uy, E. M. Gaposchkin, G. C. Light, W. W. Moore Jr., T. L. Murdock, and A. T. Stair Jr., "Midcourse space experiment: introduction to the spacecraft instruments, and scientific objectives," *J. Spacecr. Rockets* **31**, 900–907 (1994).
9. H. C. van de Hulst, *Light Scattering by Small Particles* (Wiley, New York, 1957).
10. H. C. van de Hulst, *Multiple Light Scattering* (Academic, New York, 1980).
11. S. Chandrasekhar, *Radiative Transfer* (Oxford U. Press, New York, 1950).
12. W. A. Shurcliff, *Polarized Light* (Harvard University, Cambridge, Mass., 1962).
13. C. F. Bohren and D. R. Huffman, *Absorption and Scattering of Light by Small Particles* (Wiley, New York, 1983).

14. J. E. Hansen and L. D. Travis, "Light scattering in planetary atmospheres," *Space Sci. Rev.* **16**, 527–610 (1974).
15. G. W. Kattawar, G. N. Plass, and S. J. Hitzfelder, "Multiple scattered radiation emerging from Rayleigh and continental haze layers. 1: Radiance, polarization, and neutral points," *Appl. Opt.* **15**, 632–647 (1976).
16. G. N. Plass, G. W. Kattawar, and S. J. Hitzfelder, "Multiple scattered radiation emerging from Rayleigh and continental haze layers. 2: Ellipticity and direction of polarization," *Appl. Opt.* **15**, 1003–1011 (1976).
17. E. P. Shettle and R. W. Fenn, "Models for the Aerosols of the Lower Atmosphere and the Effects of Humidity Variations on Their Optical Properties, Report No. AFGL-TR-79-0214, 1979 (Air Force Geophysics Laboratory, Hanscomb AFB, Mass.).
18. H. R. Gordon and M. Wang, "Retrieval of water-leaving radiance and aerosol optical thickness over the oceans with SeaWiFS: a preliminary algorithm," *Appl. Opt.* **33**, 443–452 (1994).
19. H. R. Gordon, "Atmospheric correction of ocean color imagery in the Earth Observing System era," *J. Geophys. Res.* **102D**, 17,081–17,106 (1997).
20. P. J. Reddy, F. W. Kreiner, J. J. Deluisi, and Y. Kim, "Aerosol optical depths over the Atlantic derived from shipboard sun-photometer observations during the 1988 Global Change Expedition," *Global Biogeochem. Cycles* **4**, 225–240 (1990).
21. Y. V. Villevalde, A. V. Smirnov, N. T. O'Neill, S. P. Smyshlyaev, and V. V. Yakovlev, "Measurement of aerosol optical depth in the Pacific Ocean and North Atlantic," *J. Geophys. Res.* **99D**, 20,983–20,988 (1994).
22. G. K. Korotaev, S. M. Sakerin, A. M. Ignatov, L. L. Stowe, and E. P. McClain, "Sun-photometer observations of aerosol optical thickness over the North Atlantic from a Soviet research vessel for validation of satellite measurements," *J. Atmos. Oceanic Technol.* **10**, 725–735 (1993).
23. A. Ivanoff, "Polarization measurements in the sea," in *Optical Aspects of Oceanography*, N. G. Jerlov and E. S. Nielsen, eds. (Academic, London, 1974) pp. 151–175.
24. G. W. Kattawar and C. N. Adams, "Stokes vector calculations of the submarine light field in an atmosphere-ocean with scattering according to a Rayleigh phase matrix: effect of interface refractive index on radiance and polarization," *Limnol. Oceanogr.* **34**, 1453–1472 (1989).